Combining SLO and OCT technology

PODOLEANU A.G.[1]

ABSTRACT

A review is presented of the research on high resolution imaging of the eye which can provide a dual display of images with different depth resolutions. The review refers to the flying spot scanning concept, widely exploited in the confocal scanning laser ophthalmoscope and recently extended to optical coherence tomography (OCT) imaging. For several reasons as presented in the paper, imaging with two different depth resolutions is useful and this has triggered the development of the dual *en-face* OCT - confocal imaging technology and of the OCT/Ophthalmoscope instrument. The dual acquisition and presentation can be performed either simultaneously (practised in the OCT/Ophthalmoscope) or sequentially. The sequential dual *en-face* OCT - confocal imaging technology can be implemented in different configurations and has specific applications. When the sequential switching is performed at the line rate of the raster frame, the display of the two images, OCT and confocal is quasi - simultaneous, in which case similar functionality is achieved to that of an OCT/Ophthalmoscope.

KEYWORDS

Optical coherence tomography, OCT, *en-face* OCT, scanning laser ophthalmoscopy, SLO, high resolution non-invasive imaging

RÉSUMÉ

Un compte-rendu de la recherche sur l'imagerie à haute résolution de l'œil est présenté, laquelle permet un double affichage d'images avec différents niveaux de résolution. Le compte-rendu se rapporte au concept de balayage par ''flying spot'', largement exploité dans l'ophtalmoscope laser à balayage confocal et récemment étendu à l'imagerie par tomographie par cohérence optique. Pour plusieurs raisons telles que présentées dans l'article, l'imagerie avec deux résolutions en profondeur différente est utile et ceci a conduit au développement de la TCO double face - technologie d'imagerie confocale et de la TCO/ophtalmoscope. La double acquisition et présentation peut être effectuée soit simultanément (pratiquée dans la TCO/ophtalmoscope) soit séquentiellement. La TCO double face séquentielle - technologie d'imagerie confocale peut être exécutée dans différentes configurations et possède des applications spécifiques. Quand la permutation séquentielle est effectuée à la vitesse d'alignement du cadre de trame, l'affichage des deux images, TCO et confocale, est quasi simultané, auquel cas une fonctionnalité similaire à celle d'une TCO/ophtalmoscope est obtenue.

MOTS-CLÉS

Tomographie par cohérence optique, OCT, OCT de face, ophtalmoscopie à balayage laser, SLO, imagerie non invasive à haute résolution

.....

[1] *Applied Optics Group, School of Physical Sciences, University of Kent, Canterbury, UK*

INTRODUCTION

Optical-coherence tomography (OCT) is a non-invasive high-resolution imaging modality which employs non-ionising optical radiation. OCT derives from low-coherence interferometry. This is an absolute measurement technique which was developed for high- resolution ranging and characterization of optoelectronic components.[1,34] The first application of the low-coherence interferometry in the biomedical optics field was for the measurement of the eye length.[7] Adding lateral scanning to a low-coherence interferometer, allows depth resolved acquisition of 3D information from the volume of biologic material.[11] The concept was initially employed in heterodyne scanning microscopy.[30] OCT has the potential of achieving high-depth resolution, which is determined by the coherence length of the source. Optical sources are now available with coherence lengths below 1 μm.[6] Using sources with extremely short coherence length, submicron depth resolution is achievable even when the microscope objective is far away from the investigated target. This is one of the most important features of OCT which explains the high level of interest for OCT in ophthalmology.

Confocal imaging was initially applied for high resolution imaging of the eye. In confocal microscopy (CM), the depth resolution is inverse proportional to the square of the numerical aperture. Therefore, the depth resolution in imaging the retina with confocal laser scanning ophthalmoscopy (SLO) [32] is limited by the combined effect of a low numerical aperture and aberrations of the anterior chamber, to 0.3 mm. Similarly, a relatively low numerical aperture of the anterior chamber limits the achievable resolution in imaging the eye lens. OCT delivers fast, non contact images of the cornea, lens and the retina with depth resolutions better than 3 μm.

OCT has mainly evolved along producing cross section images, essentially orthogonal to the plane orientation of images delivered by a microscope or by an SLO. We have shown that the flying spot concept, utilized in the SLO hardware can be combined with the OCT technology to produce *en-face* OCT images from the anterior and posterior pole. The depth resolution in CM when using low numerical aperture microscope objectives is limited while the transversal resolution in OCT is affected by random interference effects from different scattering centers (speckle). Therefore, there is scope in combining CM with OCT. The next step was natural, to provide simultaneously, quasi-simultaneously or sequentially confocal and *en-face* OCT images. The simultaneous OCT/confocal technology has been already evaluated on more than 1000 eyes with pathology, using what is now called the OCT/SLO or the OCT/Ophthalmoscope instrument.[29] A variant of this instrument, the OCT/ICG, will also be presented. This allows collection of *en-face* OCT and ICG fluorescence images from the retina. The sequential OCT-confocal imaging procedure is still in laboratory phase. This concept provides better S/N ratio in the OCT channel and better depth resolution in the confocal (SLO) channel than the OCT/SLO system. The performances of the sequential procedure will be discussed in comparison with the simultaneous procedure.

DIFFERENT SCANNING PROCEDURES

To obtain 3D information about the object, any imaging system is equipped with three scanning means, one to scan the object in depth and two others to scan the object transversally. Depending on the order these scanners are operated and on the scanning direction associated with the line displayed in the raster of the final image delivered, different possibilities exist. OCT systems, using CCD cameras or arrays of sensors or arrays of emitters eliminate the need of scanning. However, the terminology below applies in such cases as well, where the ray scanning has been replaced by electronic scanning. The scanning terminology is illustrated in figure 1 and the utilization of the three scanners in figure 2.

Longitudinal OCT (A-scan based B-scan)

B-scan images, analogous to ultrasound B-scan are generated by collecting many A-scans (Fig. 1) for different and adjacent transverse positions, as shown in figure 2 top. The lines in the raster

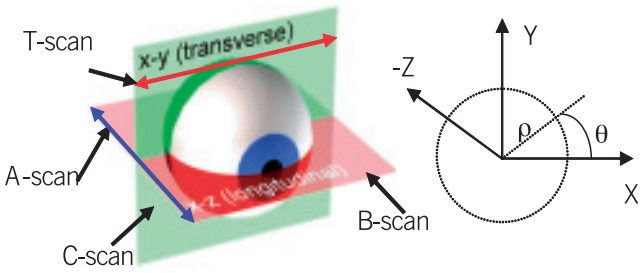

Fig. 1. Relative orientation of the axial scan (A-scan), transverse scan (T-scan), longitudinal slice (B-scan) and en-face or transverse slice (C-scan).

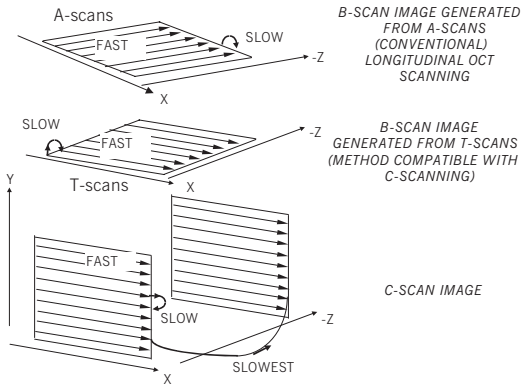

Fig. 2. Different modes of operation of the three scanners in a flying spot OCT system.

generated correspond to A-scans, i.e. the lines are oriented along the depth coordinate. The transverse scanner (operating along X or Y, or along the polar angle θ in polar coordinates in figure 1 right, with X shown in figure 2 top) advances at a slower pace to build a B-scan image. The majority of reports in literature [4] refer to this way of operation. The commercial instrument OCT3 made by Carl Zeiss Meditec operates based on this principle.
Development of the longitudinal OCT based on A-scans was facilitated by a technical advantage: when moving the mirror in the reference path of the interferometer, not only is the depth scanned, but a carrier is also generated. The information on reflectivity is superposed on a carrier signal, having a frequency equal to the Doppler shift produced by the longitudinal scanner itself (moving along the axis of the system, Z, to explore the tissue in depth). In longitudinal OCT, the axial scanner is the fastest and its movement is synchronous with displaying the pixels along the line in the raster, while the lateral scanning determines the frame rate.

En-face OCT

T-scan based B-scan

In this case, the transverse scanners (or scanner) determine(s) the fast lines in the image.[14-15] We call each such image line as a T-scan (Fig. 1). This can be produced by controlling either the transverse scanner along the X-coordinate, or along the Y-coordinate with the other two scanners fixed, or controlling both transverse scanners, along the polar angle θ, with the axial scanner fixed. The example in the middle of figure 2 illustrates the generation of a T-scan based B-scan, where the X-scanner produces the T-scans and the axial scanner advances slower in depth, along the Z-coordinate. This procedure has a net advantage in comparison with the A-scan based B-scan procedure as it allows production of OCT transverse (or 2D *en-face*) images for a fixed

reference path, images called C-scans. In this way, the system can be easily switched from B to C-scan, procedure incompatible with A-scan based OCT imaging.

C-scan

C-scans are made from many T-scans along either of X, Y, ρ or θ coordinates, repeated for different values of the other transverse coordinate, Y, X, θ or ρ respectively in the transverse plane. The repetition of T-scans along the other transverse coordinate is performed at a slower rate than that of the T-scans (Fig. 2 bottom), which determines the frame rate. In this way, a complete raster is generated. Different transversal slices are collected for different depths Z, either by advancing the optical path difference in the OCT in steps after each complete transverse (XY) or (ρ,θ) scan, or continuously at a much slower speed than the frame rate. The depth scanning is the slowest in this case.
It is more difficult to generate *en-face* OCT images than longitudinal OCT images as the reference mirror is fixed and no carrier is produced. Therefore, in order to generate T-scans and T-scan based OCT images, a phase modulator is needed in order to create a carrier for the image bandwidth, as demonstrated in reference.[9] This complicates the design and introduces dispersion. Research has shown that the X or Y-scanning device itself introduces a path modulation which plays a similar role to the path modulation created by the longitudinal scanner employed to produce A-scans or A-scan based B-scans.

Different OCT versions

There are three main OCT methods, time domain OCT (TD-OCT), Fourier domain OCT (FD-OCT) and swept source OCT (SS-OCT). In TD-OCT, an A scan is produced by varying the optical path difference (OPD) in the interferometer to output a reflectivity profile in depth. *En-face* flying spot OCT belongs to the same category where a T-scan is produced by transversally scanning the beam over the target maintaining the reference mirror fixed to output a reflectivity profile versus angle or lateral position. FD-OCT and SS-OCT output A-scans, therefore they do not allow real-time *en-face* imaging. *En-face* sections can only be obtained in FD-OCT and SS-OCT by sectioning the 3D profile obtained from several B-scan images repeated at different transverse coordinates, i.e. in a post-acquisition process only.

Simultaneous en-face oct and confocal imaging

Once the OCT image is oriented *en-face*, as described in figure 1, it has the same aspect with that of images generated by using confocal SLO.[27, 33] In both imaging technologies, the *en-face* OCT and SLO, the fast scanning is *en-face* (T-scan) and the depth scanning (optical path change in the OCT case and focus change in the CM case) is much slower (performed at the frame rate). The depth resolution in CM when using low numerical aperture microscope objectives is limited while the transversal resolution in OCT is affected by random interference effects from different scattering centers (speckle). Therefore there is scope in combining CM with OCT.
The better the depth resolution, the more fragmented the C-scan image appears. A single C-scan image from the tissue may contain only a few details and may be challenging to interpret.
In addition, the ophthalmologists have built large data bases of confocal SLO images for diseased eyes. In order to exploit this knowledge in the interpretation of the OCT transversal images, it is useful to produce simultaneously a transverse OCT and a confocal SLO image. Having a witness image, with sufficient contrast could lead to an improvement in the overall OCT imaging for retinal assessment.
In order to produce a B-scan OCT image, adjacent imaging instruments are required to guide the OCT system in directions perpendicular to the optical axis, towards the part of the tissue to be imaged.

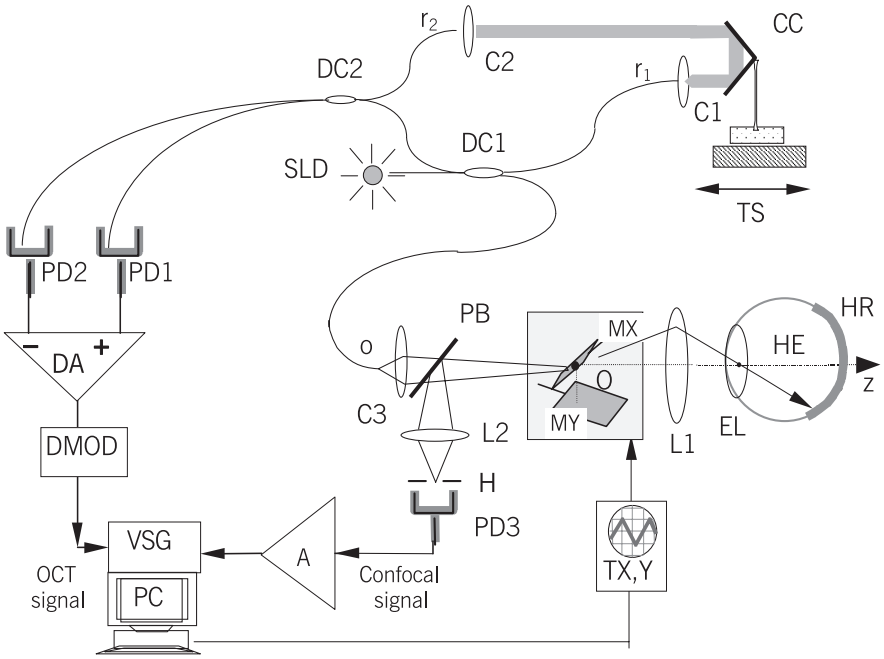

Fig. 3. Detailed schematic diagram of the OCT/Ophthalmoscope apparatus using a plate beam-splitter to divert light to a confocal receiver. SLD: Superluminescent diode; C1, C2, C3: microscope objectives; DC1, DC2: directional couplers; TS: computer controlled translation stage; CC: corner cube; M1, M2: mirrors; MX, MY: orthogonal galvanometer mirrors; TX(Y): ramp generators; DMOD: demodulation block; L1: convergent lens; PD1, PD2: photodetectors; DA: differential amplifier; PD3 and A: photodetector and amplifier respectively for the confocal receiver; H: pinhole; PB: plate beam-splitter; HE: patient's eye; EL: eye lens; HR: human retina; PC: personal computer; VSG: dual input variable scan frame grabber.

OCT/Ophthalmoscope

The four reasons above have led to a new imaging instrument [16] which blends together the two principles, OCT and CM. The combination of confocal imaging and interferometry has already been discussed in microscopy [12] and a comparison between confocal and OCT imaging through scattering media also reported.[13] However, (i) the object here is the tissue, which imposes a safety power limit and requires a special interface optics and (ii) the same low coherence source is used for both confocal and interferometer channels with implications in terms of the obtainable signal to noise ratio.

A possible configuration is shown in figure 3. Light from a pigtailed superluminescent diode, SLD, is injected into a single mode directional coupler, DC1. Light in the object arm propagates via the microscope objective C3 and plate beam-splitter PB and then enters the orthogonal scanning mirror pair, MX, MY. Lens L1 brings the fan of rays to convergence at the eye lens, EL. The reference beam is directed via microscope objectives C1 and C2 and the corner cube CC to coupler DC2. The corner cube CC is mounted on a computer controlled translation stage, TS used to alter the reference path length. The light backreflected from the object and transferred via DC1 to DC2, interferes with the reference signal in the coupler DC2. Two photodetectors, PD1 and PD2, collect the signal and their outputs are applied to the two inputs of a differential amplifier, DA, in a balanced detection configuration. The OCT signal is then demodulated in the demodulator block, DMOD which drives the OCT input of a dual variable scan frame-grabber, VSG, under control of a personal computer, PC.

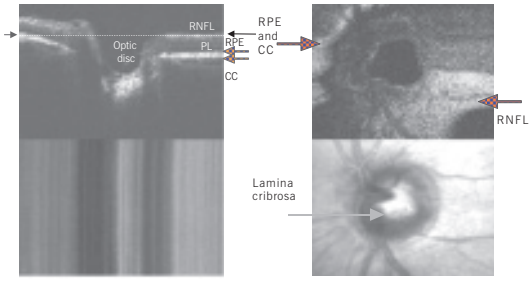

Fig. 4. Pair of images from the optic nerve acquired with the standalone OCT/confocal system. Left: B-scan regime at y = 0; Right: C-scan regime. Top images: OCT, Bottom images: confocal. The C-scan OCT image on the right is collected from the depth shown by the double arrow in the B-scan OCT image in the left. RNFL (bright): retinal nerve fiber layer; PL (dark): photoreceptor layer; RPE (bright): retinal pigment epithelium; CC (bright): choriocapillaris. 3 mm horizontal size in all images, Left: vertical coordinate in the OCT image is 2 mm depth measured in air while in the confocal image it corresponds to the acquisition time of the B-scan OCT image, 0.5 s. The lateral variations of the shades indicate lateral movements of the eye during the acquisition. Right: vertical coordinate is 3 mm in both images.

A separate confocal receiver is used [18] based on the beam-splitter BS which reflects a percentage of the returned light from the object to a separate photodetector, PD, via a lens, L2 and a pinhole, H.

Ramp generators TX,Y drive the transverse scanners equipped with the mirrors MX and MY respectively, and also trigger signal acquisition by the frame grabber.

OCT configuration with balance detection is chosen here in order to attenuate the excess photon noise, high when the OCT acquires data fast.[20]

Two types of photodetectors are employed, Silicon pin diodes for the photodetecors PD1 and PD2 in the OCT and an avalanche photodiode (APD) for the photodetector PD3 in the separate confocal receiver. The two C-scan images produced by the two channels are naturally pixel to pixel correspondent.[18] This helps with the guidance when imaging the eye.

An example of the images provided by such a system in the B and C-scan regimes of operation are shown in figure 4, from an healthy eye. The system outputs pairs of OCT and confocal images. In the left, B-scan images are shown while in the right, images obtained in the C-scan regime. The image at right, is part of a mo vie which shows an evolving OCT image as the optical path difference in the OCT is advanced, while the confocal image looks the same. The layers clearly discernible in the OCT image bears strong resemblance to histology.[10]

The combination of the C-scan OCT and confocal imaging was tested on eyes with pathology, such as: exudative ARMD, macular hole, central serous choroidopathy, RPE detachment, polypoidal choroidal vasculopathy and macular pucker.[25] A case of diabetic retinopathy is shown in figure 5 and a case of central serous retinopathy in figure 6.

The confocal image along with three other C-scan OCT images and a B-scan OCT image are shown. Here, the C-scan OCT image, at the depth D3 shows the RPE due to the curvature of the retina. The images in figures 5 and 6 show the two challenging features of the high resolution C-scan imaging: patchy fragments and display of depth structure for the tilted parts of the tissue. However, the combined display of sections in the eye along rectangular direction is extremely useful. Following the cuts along the straight lines indicated in the B-scan image, the brightness level in the corresponding part of the C-scan OCT image can be inferred.

The smaller the coherence length, the more fragmented the *en-face* OCT image appears. The usefulness of the *en-face* OCT images for the ophthalmologists is greatly improved because fragments sampled by OCT of the fundus are uniquely in correspondence with fundus images produced by the confocal channel. This channel produces images similar to those produced by a stand-alone confocal SLO. The confocal image in the dual channel OCT/confocal system was found very helpful in orientating the eye. It was much more difficult to align the eye using the

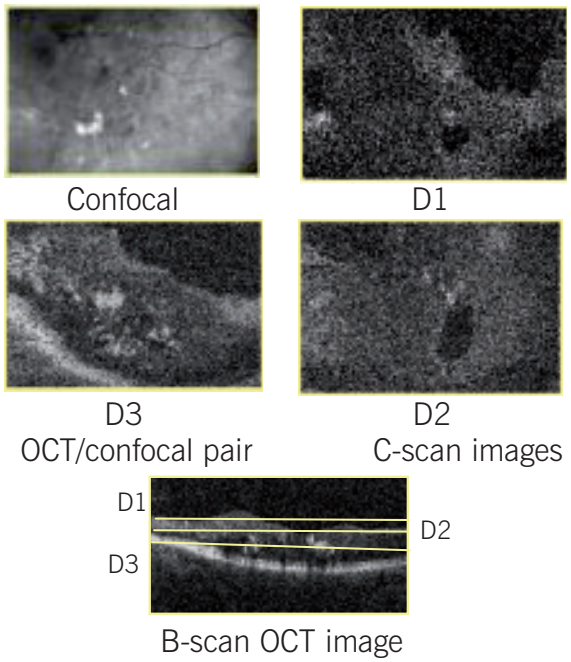

Fig. 5. Diabetic retinopathy. The lines, D1, D2, D3 in the B-scan OCT image show the depths where the C-scan OCT images have been collected from. Lateral size: 15° × 15°. Courtesy Richard Rosen, MD, Patricia Garcia, MD, Advanced Imaging Retinal Centre, New York Eye and Ear Infirmary.[20]

OCT channel alone, as an image is displayed only when at coherence, and often may not display anything, or displays a few details only.

Anterior chamber

Continuous examination from the cornea to the lens is not possible using the same optical design confocal microscope.[8] The reflection from the tear film in front of the epithelium is ~2 %. If a confocal instrument is built to image the lens, then it can be used for imaging the cornea with limited success. The low numerical aperture of the interface optics precludes separation of the different layers in the cornea from the strong reflection at the air-tear film interface. Additionally, by changing the numerical aperture means that the depth resolution at the lens depth is less than that achievable at the cornea. Thirdly, due to the low reflectivity of the transparent tissue in the anterior eye structure, there is a lack of contrast.

OCT addresses all these disadvantages and insures the same depth resolution from the cornea level up to very deep in the anterior chamber.[26]

An OCT/confocal instrument was reported for collecting images from the cornea and the anterior chamber.[22] An SLD at 850 nm which delivers 300 μW to the eye was used, depth resolution in air was slightly below 20 μm.

To visualise the cornea only, a numerical aperture of the interface optics of 0.1 was used. This gave a transversal resolution of better than 20 μm and a depth of focus of 0.25 μm in both the OCT and confocal channel (the values are larger than those theoretically expected due to aberrations). The C-scan OCT images in figure 7 show the multi-layer structure of the cornea. The top row shows sections from the epithelium.

The Bowman layer is visible in transverse section, its separation from the epithelium is transferred to the distance between the two external and internal circles. The bottom raw displays C-scan images from the endothelium.

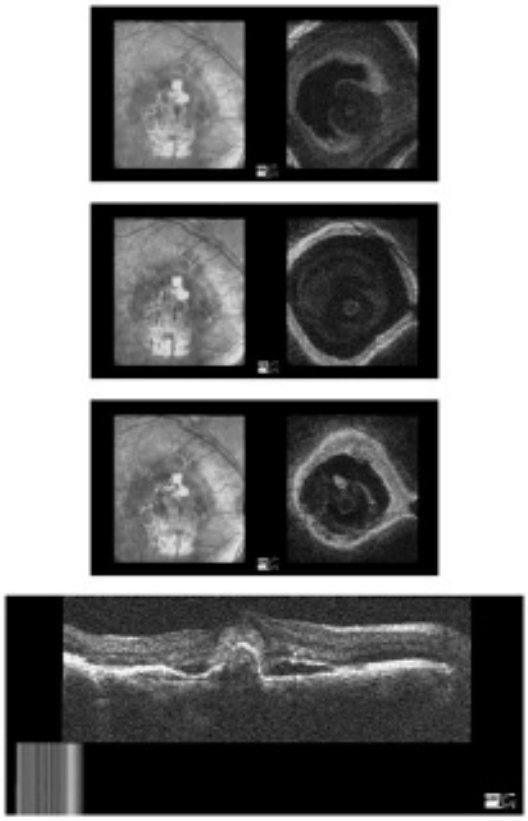

Fig. 6. Central Serous Retinopathy with a neovascular membrane. The first three rows from the top show pairs of confocal (left) and OCT (right) images. A neurosensory detachment due to fluid accumulation underneath the retina is visible. Within the serous detachment a large RPE detachment (PED) is visible. The top of the PED however is irregular and the shadowing underneath is more pronounced than it would be if it was solely a serous PED. On the B-scan image at the bottom, the irregular top of the PED is seen more clearly; the high reflective tissue is the neovascular membrane. (Courtesy of Mirjam Van Velthoven, MD, Frank Verbraak, MD, PhD and Marc de Smet, MD, PhD, Department of Ophthalmology, Academic Medical Center, Amsterdam, The Netherlands). The inset in the bottom left corner of the B-scan OCT image is the confocal image simultaneous with the OCT image.

In order to collect images in the anterior chamber as deep as from the lens, a low NA aperture interface optics was used. This gives a long depth of focus with the disadvantage that the signal strength is just sufficient to allow visualization of the most important features in the anterior chamber. Figure 8 shows a couple of pairs of C-scan images, confocal and OCT, deep in the anterior chamber, with a low NA = 0.02. The iris and the lens are visible. The images have been collected at a rate of 1 frame of pair images per second. The images at the top are the confocal images. Scanning deep in the anterior chamber, the iris appears at a depth of 3.5 mm. The irregularities of the iris rim are clearly visible at this magnification and the meshwork-like structure of the iris stroma. Then, at 4 mm depth, the lens becomes visible. The OCT images underneath show the *en-face* sections around the first Purkinje reflected spot. The offset of the lens from the center of the image indicates how sensitive C-scan imaging is at off-axis orientation in comparison with the B-scan OCT imaging. The Purkinje reflections may be useful in aligning the eye transversally, difficult to achieve when using B-scan OCT imaging alone. The first two Purkinje images are visible in the confocal channel in figure 8.

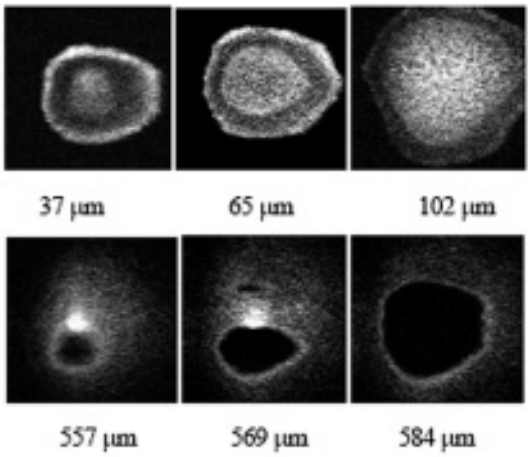

Fig. 7. En-face OCT images of the cornea (3 mm × 3 mm), three from the front and three from the back. All the depths are measured in air relative to the top of the cornea.

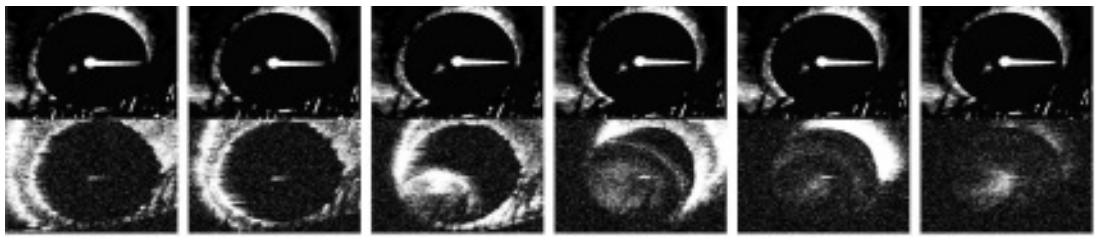

Fig. 8. Pairs of confocal (top) and OCT (bottom) images deep in the anterior chamber. Confocal images show the Purkinje reflections and the iris. Deeper, the lens is seen, offset from the optic axis, around the 3rd Purkinje image. 0.12 mm in air between the pairs. 6 mm × 6 mm transverse size.

3D IMAGING OF THE RETINA

3D imaging of the retina is already common with confocal SLO technology.[31] Proceeding with *en-face* sections in depth is widely used by ophthalmologists operating confocal SLOs. The standalone OCT/confocal can operate in the same way, however with *en-face* slices as thin as allowed by the OCT technology. To collect the reflectivity distribution from the volume of the retina, the standalone OCT/confocal system is operated in the C-scan mode collecting *en-face* images at different depths.

Ideally, the depth interval between successive frames should be much smaller than the system resolution in depth and the depth change applied only after the entire C-scan image was collected. However, in practice, to speed up the acquisition, the translation stage in the reference arm was moved continuously. For a 2 Hz frame rate, with 20 mm between frames, 60 frame-pairs from a volume in depth of 1.2 mm in air (sufficient to cover the volume of the retina around the optic nerve) can be acquired in 30 s. After acquisition, the images can be aligned transversally using the first confocal image and then the stack of OCT images or the stack of the pairs of OCT and confocal images are used to construct a 3D profile of the volume of the retina (Fig. 9). The confocal image is displayed sideways, along with the *en-face* OCT image at each depth. Then, by software means, the 3D profile can be reconstructed, in the same way reported for stacks of *en-face* images of the retina only.[21]

Different longitudinal cuts can be inferred on the sides of the reconstructed volume from the stack of *en-face* images in figure 9, similar to that shown in figure 4 top-left.

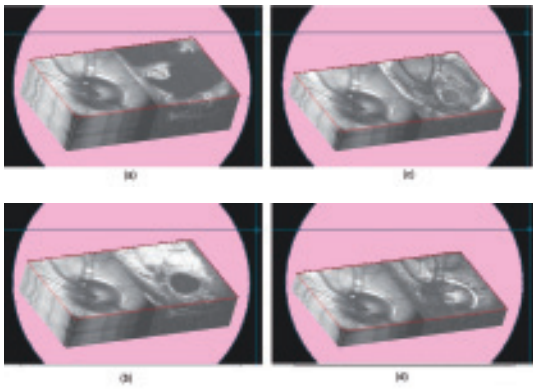

Fig. 9. 3D presentation of pairs of C-scan OCT images (right) and confocal images (left) from the optic nerve; 3 mm × 3 mm (transversal) and 1.5 mm (depth in air).

SIMULTANEOUS OCT AND FLUORESCENCE IMAGING

Once a confocal channel is added to the OCT channel, all known applications of confocal microscopy can be implemented on the confocal channel while benefiting from the simultaneous information offered by the OCT channel. One of such possibility is to tailor the confocal channel to provide information on the fluorescence of the tissue under investigation. A simultaneous OCT/fluorescence imaging instrument has been produced which provides a fluorescence image of indocyanine green (ICG) at the same time with an *en-face* OCT image from the eye fundus.[3-4] The same optical source, a superluminescent diode at $\lambda_0 = 793$ nm center wavelength was employed to produce the OCT signal as well as to excite the ICG. The beam-splitter BS in figure 3 is a dichroic filter which separates the ICG excitation (and the OCT signal) from the fluorescence.
The system can operate in different regimes. In the B-scan OCT regime only one galvo-mirror of the galvanometer scanning pair is driven with a ramp at 500-1000 Hz and the translation stage is moved for the depth range required in 1 s. In this case, an OCT B-scan image is produced either in the plane (x,z) or (y,z).
In the C-scan OCT regime, one galvo-scanner is driven with a ramp at 500-1000 Hz and the other galvo-scanner with a ramp at 1-5 Hz. In this way, a C-scan image, in the plane (x,y) is generated, at constant depth. Then the depth is changed by moving the translation stage in the reference arm of the interferometer and a new C-scan image is collected.
Images of the fundus of a patient with a choroidal neovascular membrane are shown in figure 10. In (a), the image on the left shows full ICG filling of the retina and choroidal vessels with a comma-shaped hyperfluorescent lesion within the central foveal dark zone that represents a neovascular membrane. The corresponding C scan OCT on the right reveals a slight posterior tilt of the scan to the right such that the vitreous is represented by the black region on the left. The adjacent bright circular region with attached arms represents the vitreous-retinal interface - nerve fiber layer region. It surrounds a gray region of concentric circles, which correspond to a serous elevation enveloping the neovascular complex. The double line of the retina-RPE interface in the upper right. (b) shows the smaller vascular structures which become less distinct later in the ICG transit sequence. The C-scan OCT shows that the tilt has shifted in this pair such that the choroid is captured in the upper left corner and the vitreous is in the lower right. The larger apparent size and more central location of the neovascular membrane in relation to the surrounding retinal structures places the depth of this cut somewhere near the mid-thickness of the retina. The image in (c) is a B-scan image. The two small insets in the corners are confocal images. That in the left corner is the image delivered by the confocal channel, while performing

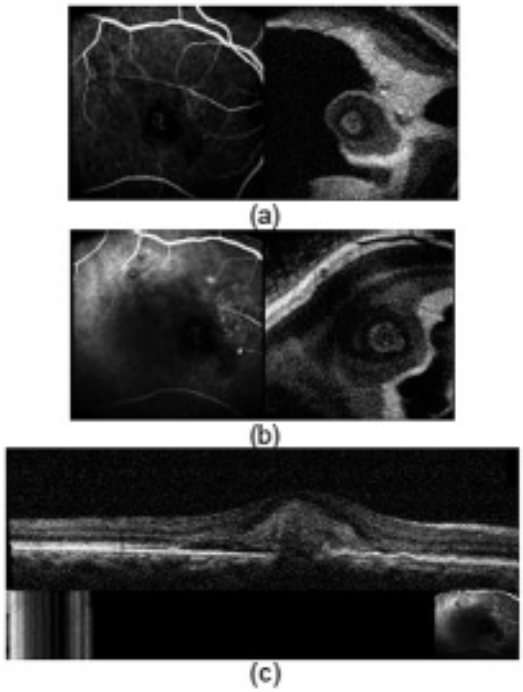

Fig. 10. Images of the fundus of a patient with a choroidal neovascular membrane. Pairs of e*n face* OCT (right) and ICG fluorescence (left) in the post-injection phase at (a) 10 sec, (b) 15 sec. Lateral size, 260 × 260. Axial distance between OCT slices ~200 mm. (c): B-scan image, the same lateral size, 26o as the images above, the depth range 1.5 mm in air. Courtesy Richard Rosen, MD, Patricia Garcia, MD. Advanced Imaging Retinal Centre, New York Eye and Ear Infirmary.[26]

OCT B-scan imaging. That in the right corner is the image delivered by the confocal channel in the C-scan regime, just before switching the system into the B-scan regime.
Aside from the obvious advantages of cost savings and reduction of irradiation time of the patient's eye, the acquisition of simultaneous corresponding images leads to an unique correlation of anatomic features with vascular functional changes.

SEQUENTIAL OCT AND CONFOCAL IMAGING

As explained in reference [16] the confocal receiver core of a two-directional coupler OCT configuration could not be exploited to generate an image due to the residual signal reflected by the fiber end. Even if the fiber end is cleaved at an angle, its reflection is 10^{-5}. This is comparable or larger than the signal reflected by the retina. Therefore, a novel configuration [24] was devised (as shown in figure 11) where the fibre end reflection was totally eliminated by employing a plate beam-splitter while maintaining the second optical splitter in fibre. In this way, two *en-face* imaging channels of different depth resolution are implemented without diverting any signal from the object arm to a supplementary confocal receiver. The plate beam-splitter separates light from the optical source, a superluminiscent diode, into a reference beam and an object beam.
In the object arm, a pair of galvanometer scanners is used to scan the beam across the eye via interface optics. The reference path is adjusted using a micrometer precision PC controlled translation stage. The reference beam and the beam returned from the object via the interface optics, galvanometer scanners and plate-beam-splitter interfere in the 50/50 single mode directional coupler DC. The outputs of the DC lead to two photodetectors, PD1 and PD2. Either of the two regimes of operation, OCT or confocal, can be selected by (i) simply flipping an opaque screen

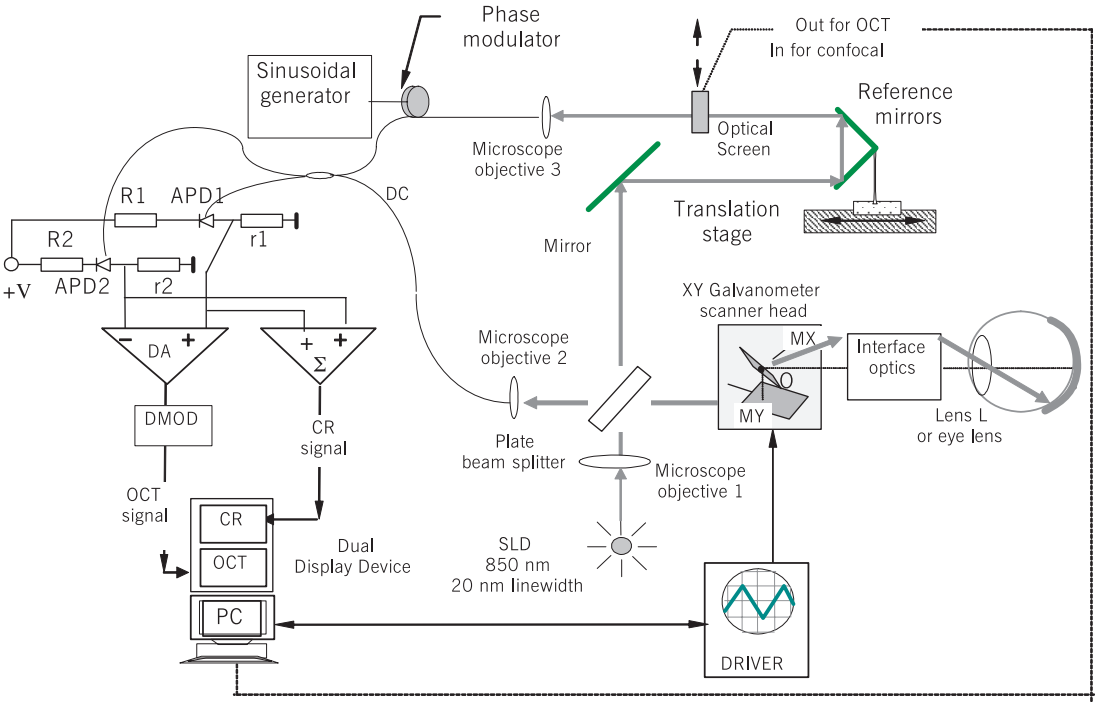

Fig. 11. Schematic diagram of the sequential OCT confocal system.

into and out of the path of the reference beam of the interferometer and (ii) exploiting the unique feature of self adjusting gain of avalanche photodiodes depending on the illumination level. By blocking the reference path, the two APDs receive optical signal from the object only. As a result of a much lower photodetected current, the voltage drop on resistors R1 and R2 is insignificant, the voltages across the APDs increase up to the avalanche threshold resulting in a corresponding increase in the gain of the two APDs. The two detected signals collected from resistors r1 and r2 are added up in the summing amplifier, Σ. The two APDs and the summing block Σ act as a confocal signal receiver (CR).

To activate the OCT channel, the opaque screen is out and due to the relative large power of the reference beam, the APD photocurrent is high. Large voltage drops appear on the resistors R1 and R2 in series with the APDs, which bring the voltages across the APDs below the level required for avalanche. In this regime, the APDs operate with a gain close to unity, similar to pin diodes. The difference of the two photodetected currents is available at the output of the differential amplifier DA, as input to the OCT channel. The S/N ratio in the OCT channel obtained with the two Silicon APDs in the regime described was similar to that obtained using a balanced receiver using Silicon pin photodetectors. The DA output signal is further demodulated in the demodulator block DMOD to provide the OCT signal. A dual channel variable scan frame grabber (Bit Flow Raven, 8-bit, 40 MHz) is used to display the two images, OCT and confocal. The fiber aperture of the directional coupler DC acts as a confocal restricting aperture, which depends on the fibre and on the interface optics used, but is generally 5-10 mm for single mode fibre. This determines a very good depth sectioning interval of the confocal channel and acts as the confocal receiver core of the OCT channel. However, the signal collected is smaller than in the previously reported configuration using a pinhole. To evaluate the FWHM profile of the confocal sectioning interval, a mirror as the object was used, properly aligned to return maximum signal. This was shifted axially through focus while recording the signal strength. Using a lens of 2 cm

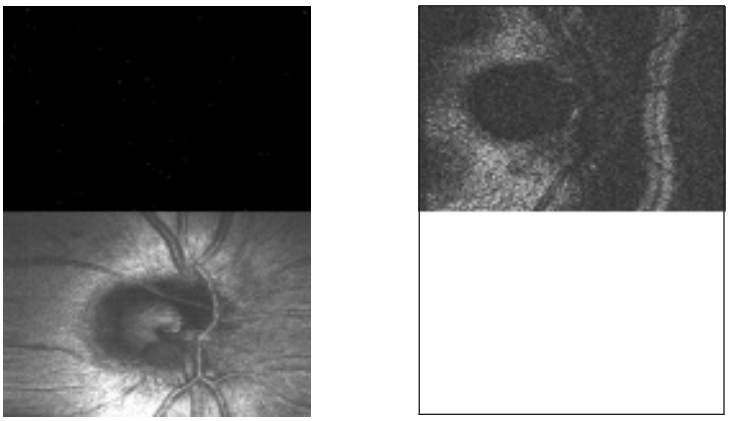

Reference arm blocked Opaque screen removed

Fig. 12. Pairs of sequential OCT (top) - confocal (bottom) images from the optic nerve in vivo. Lateral size ~ 3 mm × 3 mm. The OCT image is collected at a depth halfway between the retinal nerve fiber layer and lamina cribrosa

to mimic the anterior eye leads to 0.23 mm, however, as known, due to the eye aberrations, the FWHM of the depth profile of the confocal SLO cannot be better than 0.3 mm.
To scan the object, the X-galvoscanner was driven with ramps of 700 Hz while the Y-galvoscanner with ramps of 2 Hz. The power to the object was 180 mW. The phase modulation mainly due to the X-galvoscanner was employed to generate the OCT image, although for small size images, a fiber phase modulator driven by a sinusoidal generator at 33 kHz was also provided. A discussion on the role of each phase modulation depending on the image size is presented in reference.[17]
Pairs of OCT (top) and confocal (bottom) images are shown in figure 12 illustrating the operation of the system. The confocal images, when the screen is removed, are completely white due to the saturation of the amplifying block chain (summing amplifier Σ and the frame grabber input). When the reference arm is blocked, a confocal image is visible at the bottom in the pair of images in the left column. The confocal image is artifact free, with no reflections from the cornea or the intermediate lenses.
The toggle between the two regimes of operation depends mainly on how fast the APDs can be switched from low gain below avalanche to high gain in the avalanche regime. For fast APDs, the switching time could be of the order of a few ns. However, in order to maintain a good signal to noise ratio, the bandwidth of the electronic chain following the APDs is restricted to the minimum required to process the image bandwidth. Consequently, when switching between the two regimes of operation, the signal in each channel transits between different magnitudes corresponding to the image intensity in the two regimes. This transitory regime takes place over a time given by the inverse of the channel bandwidth.
When switching from OCT to confocal regime, the electronics in the confocal channel also has to change from saturation to a linear regime of operation. This requires some recovery time. However, in our configuration these transit times were much less than the duration of a frame, 0.5 s. We used a two channel frame grabber for convenience, however a single channel frame grabber could also be employed if means are provided for switching the outputs of the OCT and confocal channels in a synchronous manner with flipping the screen.
One of the main difference between the configuration in figure 3 and that in figure 11 is that the confocal receiver uses single mode optical fibre. This determines better rejection of stray reflections in the system and better selection in depth in the confocal channel. Therefore, this configuration seems very attractive for investigations of the cornea, where similar depth resolutions are achievable in the two channels in comparison with the imaging of retina case.

QUASI-SEQUENTIAL IMAGING WITH TWO DIFFERENT DEPTH RESOLUTIONS

So far, the pair of two images with different depth resolution have been generated using two different technologies, OCT and confocal. An image of similar aspect to that generated by the confocal channel could be obtained using OCT principles. In the past we evaluated the possibility of *en-face* OCT imaging with adjustable depth resolution. Adjusting the coherence length, the depth sampling interval can be altered up to that of a confocal SLO and beyond. In comparison to the two previously presented concepts, dual imaging with different depth resolutions is obtained manipulating the properties of the optical source. The instrument shown in figure 13 generates quasi-simultaneously two OCT images with different depth resolution,[23] instrument termed in what follows as OCT1/OCT2. The system is illuminated by two light sources of different coherence lengths. In a typical *en-face* OCT system, a pair of galvanometer scanners is employed to scan the target transversally. One mirror is driven at a much higher rate than the other and its movement determines the line in the final raster while the slower mirror movement determines the frame. As shown in figure 13, a triangle signal is used to drive the scanner responsible for the line movement. During the first half cycle (ascending slope) of the triangle signal, the system is illuminated by one source. During the second half cycle (descending slope) of the triangle waveform, the first source is switched off and the system is illuminated with the second source only. The two light sources are toggled on and off synchronously with the *en-face* scanning. In our system, the line is horizontal and the frame movement is vertical. The frequency of the horizontal scan signal generated by the horizontal signal generator (HSSG) (which drives the horizontal scanning mirror M_x responsible for the line movement) determines the duration that each source is on during a cycle. Given a line scan frequency of 700 Hz, each source is on for only half (0.71 ms) of a full line scan cycle, much less than the observer eye can follow. Therefore, the two OCT images are quasisimultaneous. We used a 2 Hz saw-tooth waveform generated by the vertical scan signal generator (VSSG).

The target images captured by the system are time-inverted with respect to the median of the frame grabber display window.

Frame and line synchronization TTL pulses from the generators HSSG and VSSG (signals TTLH and TTLF respectively) are fed to the dual input frame grabber. The TTLH signal drives the frame grabber line synchronization input and triggers the operation of the block DELAY. This is inserted into the control line to compensate the scan delay due to the inertia of the galvanometer scanner spinning the mirror M_X. To make sure that when one source is on the other is off, an inverter was used to drive one of the optical sources.

The system employed a SLD at 850 nm, linewidth 19.4 nm and a three-electrode laser at 858 nm with linewidth variable between 1 and 1.8 nm. Assuming a Gaussian power spectrum shape, the FWHM line-width gives a coherence length of ~ 33 μm for the SLD source and variable between 350 and 650 μm for the three electrode laser respectively. The maximum power at the target we could obtain from the three electrode laser was 70 μW respectively. Although the SLD source was more powerful, its power was deliberately limited to a similar value to obtain similar brightness for the images generated by the two sources driving the system. A single mode coupler was used to send light from the two sources to the OCT.

Due to the fact that each source is on while the other is off, there are no safety level concerns. Evaluation of the safety level for the eye is presented in reference [28]. Using a lateral pixel size of ~ 15 μm, a line of 3 mm covering the object (as a minimum to scan the optic disk), the line rate of 700 Hz and the frame rate of 2 Hz, investigation with 120 μW is allowed for many hours[32] at 820-850 nm.

En-face OCT images from the optic nerve in vivo are shown in figure 14. The coherence length of the three electrode laser was adjusted for the OCT channel to give 300 μm depth resolution in air. Pairs of *en-face* OCT images are shown at different depths in the retina, separated by 190 μm.

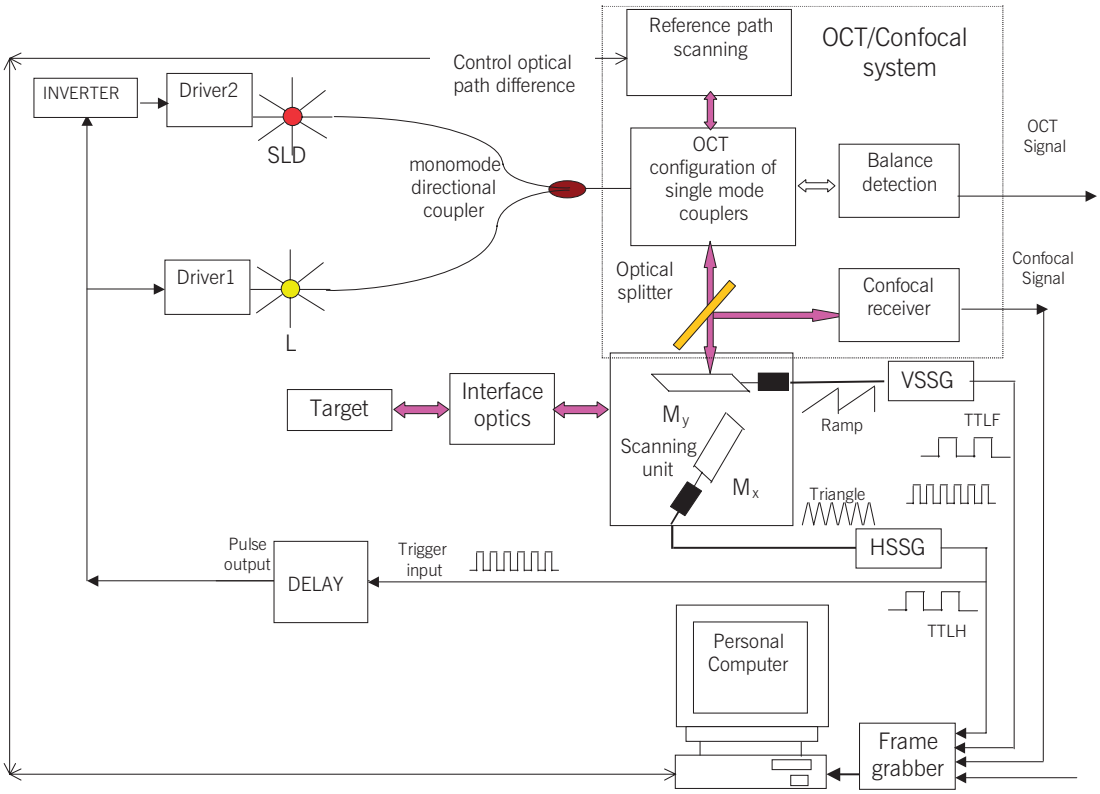

Fig. 13. Block diagram of the OCT system with quasi-simultaneous image display capabilities and dual source input of different coherence length: SLD: superluminescent diode; L: laser diode or three electrode laser device; $M_{x,y}$: horizontal and vertical scanning mirrors, VSSG: vertical scanner driving signal generator; HSSG: horizontal scanner driving signal generator; Delay: variable width pulse generator.

The OCT images collected with the SLD on the right show sharp cuts in depth due to the inclination of the coherence surface at the back of the eye. The bright arc is the retinal pigment epithelium and the choriocapillaris which show up as the brightest layers in any longitudinal OCT images of healthy retina. The same cut appears more diffuse and occupies a larger area on the OCT image obtained with the three electrode laser on the left. The depth resolution of the OCT image generated with the three electrode laser is sufficient to separate the lamina cribrosa from the retinal nerve fiber layer, as seen by comparing the top and the bottom images. The difference in depth resolution is demonstrated by the images in the bottom row where at the same depth, the image on the right does not display any traces of the lamina cribrosa (due to higher depth resolution) which is visible in the image on the left.

CONCLUSIONS

In ophthalmology, OCT has allowed imaging of the back of the eye with more than 100 times better depth resolution than that using confocal SLOs. However, when orienting the OCT image *en-face*, it is more difficult to interpret it than a cross-section image (B-scan). Penalties are incurred using *en-face* OCT imaging when attempting to improve the depth resolution by reducing the coherence length of the source, namely: fragmentation of the image, increased difficulty in bringing the object to coherence and increased sensitivity to movements and vibrations. A wider sectioning depth interval alleviate these problems.

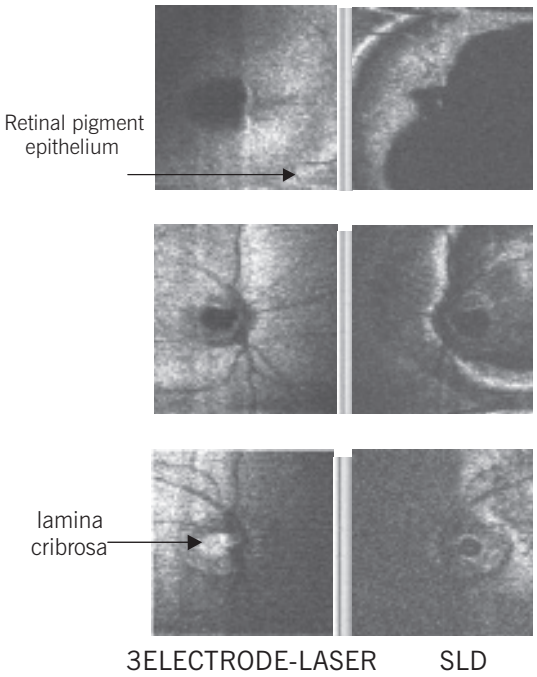

Fig. 14. Quasi-simultaneous mirror-symmetric *en-face* OCT images of the optic nerve in vivo at different depths. Difference in depth between the succesive pairs: 190 mm. Lateral size: 3 mm × 3 mm.

In order to help with target positioning and improve image interpretation, different solutions have been adopted. One such solution consisted in combining *en-face* OCT with confocal microscopy in a dual simultaneous channel OCT/confocal system (the OCT/Ophthalmoscope). When imaging the retina, the confocal channel operation was similar to that of a standard SLO. The confocal channel has a much larger depth resolution than the OCT channel and therefore the images look continuous and are less susceptible to eye movements. Therefore, the dual presentation allows the OCT-sampled fragments from the eye fundus to be placed in a unique correspondence with fundus images displayed by the confocal channel. Initial human studies have shown that the dual display is essential for guidance, subsequent alignment and processing of the stack of *en-face* images prior to the construction of the 3D data of the volume investigated. Such systems are now used for imaging of both posterior and anterior pole. A similar configuration was used for simultaneous OCT-fluorescence imaging when the confocal channel was tuned to the fluorescence of the ICG spectrum.

However, the incorporation of a confocal channel in the system was performed at the expense of the signal to noise ratio in the OCT channel, as some of the signal returned by the object had to be diverted to a confocal receiver. The confocal channel taps some of the already weak signal returned from the tissue, which results in a lower achievable signal to noise ratio in the OCT channel. For instance, when 10 % is tapped, the loss in the OCT channel is more than 19 %. Therefore we looked into other configurations with better efficiency in using the back-scattered signal in the OCT channel. A possible solution in this respect is offered by sequential operation of the OCT and confocal regime of operation. A system operating accordingly was presented. A channel of large depth resolution is implemented using the confocal receiver at the core of the OCT. In order to make this possible, a special hybrid OCT configuration is devised in order to minimize the stray reflection in the object arm of the interferometer. The special configuration allows a choice between operating in the confocal or in the OCT regime. In this way, two *en-face* images are produced and displayed sequentially, one OCT and the other confocal. All signal re-

turned from the eye is used sequentially in each channel, OCT and confocal. The two images have depth resolutions, at present, of better than 20 μm and over 0.3 mm respectively. Switching between the two types of image is performed by flipping an opaque screen in the reference arm coupled with the self adjusting gain operation of avalanche photodiodes in the receiver.
Finally, an alternative method for the dual display of *en-face* images with different depth resolution was presented. This employs OCT principles in both channels, but each channel using a different optical source. Therefore, the instrument based on this method is termed as OCT1/OCT2. This simplifies the optical configuration with some increase in the complexity of the electronics processing. The method does not require tapping into the OCT signal and both channels perform OCT. The main improvement is in the channel of poorer depth resolution (comparing the performances of the confocal channel in a simultaneous OCT/confocal configuration with the channel of poorer depth resolution in the OCT1/OCT2 configuration). For similar depth resolution, the glare and stray reflections in the channel of poorer depth resolution are better eliminated in the dual OCT configuration. The low depth resolution OCT channel could obviously replace the confocal channel and be employed for optimum positioning of the object to be imaged, as more details can be seen in the *en-face* OCT image generated by this channel.
However, there are fundamental differences between the implementation of a confocal and OCT channel to produce a coarser depth resolution image. In the confocal channel, the coarser the depth resolution, the better the signal to noise ratio, especially due to the increase in the signal (limitation exists in this case too, as stray reflections from optical components increase the noise when the pinhole is enlarged). In OCT however, there are two competing effects due to the excess photon noise characteristic for low coherence sources, an increase in the coherence length is associated with an increase in the noise. By enlarging the coherence length, more scattering points in depth in the tissue contribute to the signal for a given pixel in transversal section, which leads to an increase in the signal.
It should be said that the design of the OCT1/OCT2 instrument derives from studies on imaging the tissue with adjustable depth resolution.[19] This is required by *en-face* OCT only. While B-scan imaging demands the highest achievable depth resolution, and 2 μm depth resolution was reported from the cornea and 3 μm from the retina,[5] resolution of 50 to 200 μm has applications in the guidance of the *en-face* imaging of the retina.
The main objective of the research on implementing such a variety of dual channel imaging configurations is to obtain a steady, easy to interpret overall image to guide the high resolution, fragmented *en-face* OCT image. As mentioned above, the *en-face* OCT image may display tiny fragments and also may be warped due to the curvature of the retina and eye movements, which make the image interpretation difficult. The configurations presented are possible solutions to address these problems, where by different means, OCT or confocal, a coarser depth resolution image is generated. Also, generation of such a witness image with larger depth resolution serves to the alignment of stacks of *en-face* OCT images. This is allowed due to the unique design of all the configurations reviewed here, where both channels share the transverse scanner and therefore, the two images generated are pixel to pixel correspondence. This alignment can be performed on the set of coarser images obtained based on either the confocal or OCT principle.

ACKNOWLEDGMENTS

The author acknowledges the support of EPSRC, UK, New York Eye and Ear Infirmary, NY, USA, Ophthalmic Technology Inc., Toronto, Canada, Pfizer Sandwich, UK and Superlum Moscow, Russia.

REFERENCES

(1) AL-CHALABI S.A., CULSHAW B., DAVIES D.E.N. – Partially coherent sources in interferometric sensors. First International Conference on Optical Fibre Sensors, 26-28 April 1983, I.E.E. London. 1983; 132-135

(2) AMERICAN NATIONAL STANDARD FOR THE SAFE USE OF LASERS – ANSI Z 136.1, 1993. Laser Institute of America, New York, NY 1993
(3) DOBRE G., CERNAT R., ROSEN R.B., PODOLEANU A.G. – Simultaneous OCT/ICG fluorescence imaging system for investigations of the eye fundus, Coherence Domain Optical Methods and Optical Coherence Tomography, Conference in Biomedicine VIII. Tuchin V.V., Izatt J.A., Fujimoto J.G. (eds.). Proc. SPIE. 5316. 5, 5, 1-6
(4) DOBRE G., ROSEN R.B., PODOLEANU A.G. – Simultaneous OCT/ICG fluorescence imaging system for investigations of the eye fundus. Opt Lett 2004 (in press)
(5) DREXLER W., MORGNER U., GHANTA R.K., KARTNER F.X., SCHUMAN J.S., FUJIMOTO J.G. – Ultrahigh-resolution ophthalmic optical coherence tomography. Nature Medicine 2001; 7: 502-507
(6) DREXLER W. – Ultrahigh-resolution optical coherence tomography. J Biomed Opt 2004; 9: 47
(7) FERCHER A.F., MENGEDOHT K., WERNER W. – Eye length measurement by interferometry with partially coherent light. Opt Lett 1988; 13: 186-189
(8) FURRER P., MAYER J.M., GURNY R. – Confocal microscopy as a tool for the investigation of the anterior part of the eye. Journal of Ocular Pharmacology and Therapeutics 1997; 13: 559-578
(9) HITZENBERGER C.K. – Three-dimensional imaging of the human retina by high-speed optical coherence tomography. Opt Express 2003; 11: 2753-2761
(10) http:www.udel.edu/Biology/Wags/histopage/colorpage/cey/cey.htm
(11) HUANG D., SWANSON E.A., LIN C.P., SCHUMAN J.S., STINSON W.G., CHANG G.W., HEE M.R., FLOTTE T., GREGORY K., PULIAFITO C.A., FUJIMOTO J.G. – Optical coherence tomography. Science 1991; 254: 1178-1181
(12) JUSKAITIS R., WILSON T. – Scanning interference and confocal microscopy. J Microscopy 1994; 176: 188-194
(13) KEMPE M., RUDOLPH W., WELSCH E. – Comaparative study of confocal and heterodyne microscopy for imaging through scattering media. JOSA 1996; 13: 46-52
(14) PODOLEANU A.G., DOBRE G.M., WEBB D.J., JACKSON D.A. – Coherence imaging by use of a Newton rings sampling function. Opt Lett 1996; 21: 1789-1791
(15) PODOLEANU A.G., DOBRE G.M., JACKSON D.A. – En-face coherence imaging using galvanometer scanner modulation, Opt Lett 1998; 23: 147-149
(16) PODOLEANU A.G., JACKSON D.A. – Combined optical coherence tomograph and scanning laser ophthalmoscope. Electron Lett 1998; 34: 1088-1090
(17) PODOLEANU A.G., SEEGER M., DOBRE G.M., WEBB D.J., JACKSON D.A.., FITZKE F. – Transversal and longitudinal images from the retina of the living eye using low coherence reflectometry. J Biomed Optics 1998; 3: 12-20
(18) PODOLEANU A.G., JACKSON D.A. – Noise Analysis of a combined optical coherence tomography and confocal scanning ophthalmoscope. Appl Opt 1999; 38: 2116-2127
(19) PODOLEANU A.G., ROGERS J.A., JACKSON D.A. – OCT En-face Images from the Retina with Adjustable Depth Resolution in Real Time. IEEE J of Sel Topics in Quant Electron 1999; 5 (4): 1176-1184
(20) PODOLEANU A.G. – Unbalanced versus balanced operation in an OCT system. Appl Opt 2000; 39: 173-182
(21) PODOLEANU A.G., ROGERS J.A., JACKSON D.A., DUNNE S. – Three dimensional OCT images from retina and skin. Opt Express 2000; 7 (9): 292-298
(22) PODOLEANU A.G., ROGERS J.A., DOBRE G.M., CUCU R.G., JACKSON D.A. – En-face OCT imaging of the anterior chamber. Proc SPIE 2002; 4619: 240-243
(23) PODOLEANU A.G., CUCU R.G., ROSEN R.B., DOBRE G.M., ROGERS J.A., JACKSON D.A. – Quasi-simultaneous OCT en-face imaging with two different depth resolutions. J Phys D: Appl Phys 2003; 36: 1696-1702
(24) PODOLEANU A.G., DOBRE G.M., CUCU R.G., ROSEN R. – Sequential OCT and Confocal Imaging. Opt Letters 2004; 29: 364-366
(25) PODOLEANU A.G., DOBRE G.M., CUCU R.G., ROSEN R., GARCIA P., NIETO J., WILL D., GENTILE R., MULDOON T., WALSH J., YANUZZI L.A., FISHER Y., ORLOCK D., WEITZ R., ROGERS J.A., DUNNE S., BOXER A. – Combined Multiplanar Optical Coherence Tomography and Confocal Scanning Ophthalmoscopy. J Biomed Opt 2004; 9: 86-93
(26) RADHAKRISHNAN S., ROLLINS A.M., ROTH J.E., YAZDANFAR S., WESTPHAL V., BARDENSTEIN D.S., IZATT J.A. – Real-time optical coherence tomography of the anterior segment at 1310 nm. Arch Ophthalmol Chic 2001; 119: 1179-1185

(27) RAJADHYAKSHA R., ANDERSON R., WEBB R. – Video-rate confocal scanning laser microscope for imaging human tissues in vivo. Appl Opt 1999; 38: 2105-2115
(28) ROGERS J.A., PODOLEANU A.G., DOBRE G.M., JACKSON D.A., FITZKE F.W. – Opt Express 2001; 9: 476
(29) ROSEN R.B., PODOLEANU A.G., DUNNE S., GARCIA P. – Optical coherence tomography ophthalmoscope. In: Ciulla T.A., Regio C.D., Harris A. (eds.) Retina and optic nerve imaging. Lippincot Williams & Wilkins, Philadelphia 2003; 119-136
(30) SAWATARI T. – Optical heterodyne scanning microscope. Appl Optics 1973; 12: 2766 - 2772
(31) WEBB R.H., HUGHES G.W., DELORI F.C. – Confocal scanning laser ophthalmoscope. Appl Optics 1987; 26: 1492-1499
(32) WEBB R.H. – Scanning laser ophthalmoscope. In: Masters B.R. (ed.) Noninvasive diagnostic techniques in ophthalmology. Springer-Verlag, New York 1990; 438-450
(33) WILSON T. – Confocal microscopy. Academic Press, London 1990
(34) YOUNGQUIST R.C., CARR S., DAVIES D.E.N. – Optical coherence-domain reflectometry: a new optical evaluation technique. Opt Lett 1987; 12: 158-160

.....

Corresponding address:

Adrian Podoleanu, PhD
School of Physical Sciences
University of Kent
Giles Lane
Canterbury CT2 7NH
UNITED KINGDOM
Phone: ++ 44 1227 82 3272 (3272)
Email: ap11@kent.ac.uk